International Journal of
Geo-Information

MDPI

Article

Fire Scenario Zone Construction and Personnel Evacuation Planning Based on a Building Information Model and Geographical Information System

Qiang Yang *, Xu Zhang, Zhongren Zhang, Longjiang He, Xiaojie Yan and Jiaming Na

College of Civil Engineering, Nanjing Forestry University, Nanjing 210037, China; xuzhang@njfu.edu.cn (X.Z.); zhongrenzhang@njfu.edu.cn (Z.Z.); longjianghe97@njfu.edu.cn (L.H.); xiaojieyan@njfu.edu.cn (X.Y.); jiaming.na@njfu.edu.cn (J.N.)

* Correspondence: qiangyang@njfu.edu.cn

Abstract: The spatial–temporal simulation of fire disasters and evacuation route planning are important research fields for urban emergency responses and are primary tasks that answer complex questions after fires break out. The increasing demand for refined building information models will sharply increase the calculated and analyzed quantity. This demand presents a challenge for fire emergency responses based on massive building information. In this paper, the principle of the realistic worst case (RWC) is introduced into fire simulation and evacuation route planning. Taking the library of the Nanjing Forestry University as the study object, the spatial–temporal characteristics of the influential environmental factors of the fire are simulated, such as the meteorological elements, building structure, and building skin. The scenario zones that are relatively prone to fire are selected using an overlay analysis across the four seasons. Then, the risk threshold for evacuating personnel is analyzed in the fire zone according to international standards and firefighting criteria. Specific parameters are determined based on the analysis of the above. The growing trends for fires across the four seasons are simulated with scenario zones as the starting positions and incorporate factors such as temperature, carbon monoxide, and smoke. Lastly, a life safety assurance path (LSAP) for personnel evacuation is designed based on an indoor road network and path search algorithm. The evacuation planning result is compared with the traditional shortest-time path and shortest-distance path. Based on the study results, fire scenario zones can improve the speed and operating efficiency of spatial–temporal simulation models of fire and can also support path planning and design for emergency responses.

Keywords: building information model; environmental factors; fire scenario; spatial–temporal simulation; personnel evacuation

Citation: Yang, Q.; Zhang, X.; Zhang, Z.; He, L.; Yan, X.; Na, J. Fire Scenario Zone Construction and Personnel Evacuation Planning Based on a Building Information Model and Geographical Information System. *ISPRS Int. J. Geo-Inf.* **2022**, *11*, 110. https://doi.org/10.3390/ijgi11020110

Academic Editors: Luigi Barazzetti, Mattia Previtali, Branka Cuca and Wolfgang Kainz

Received: 2 December 2021
Accepted: 2 February 2022
Published: 3 February 2022

1. Introduction

Rapid global urbanization has promoted the development of three-dimensional urban spaces, both aboveground and underground. The number of megastructures such as skyscrapers, shopping malls, and superdeep underground buildings has increased significantly in recent years [1,2]. These buildings allow a very high density of people to live and work in an area. Additionally, an increasing number of built megastructures are facing over-aging problems and lack regular maintenance. These issues bring about challenges in terms of fire emergency prevention and control. On the one hand, the rapid onset of fire can produce dangers and threaten personal safety due to heat, smoke, and toxic gas [3]. On the other hand, indoor spaces containing a high density of people cause uncertainties in fire scenarios. A reliable rescue and evacuation plan is, thus, of great importance for megastructures.

Recently, personal awareness of fire protection has gradually increased, while fire extinguishers have steadily improved. These improvements dramatically decrease serious fire accidents [4]. However, building fire prevention should be a priority since fire might lead to significant disasters with inappropriate planning. Official standards or laws for fire protection are published by many government and international organizations, e.g., GBJ16 in China, NFPA 92 in the USA, BSI in the UK, and AS1530 in Australia. An effective warning system before a fire should be installed to minimize the damage during a fire process [5]. A reasonable and scientific warning system should involve temporal and spatial simulations of building fires, influenced by the building structure, materials, local environment, and many other fire factors [6,7]. Moreover, the occurrence and development mechanism of a fire accident should also be taken into consideration. These factors can be revealed based on a fire scenario simulation [7]. Furthermore, an accurate fire scenario simulation can also supply response strategies for building fire prevention and firefighting [5,8].

For building fire simulations and evaluations, previous studies have mainly focused on fire development theory, building structure and form, building materials, influential factors, process models, emergency responses, and standards [2,5,9–13]. The numeric fire scenario simulation approach mainly contains three types, e.g., network-based, regional, and zonal [14]. Yang et al. (2012) simulated fire development trends for different locations using temperature measurements in interior building corridors, elevators, and staircase exits [1]. Bi et al. (2013) adopted the finite element analysis method to analyze the behavior of a reinforced-concrete-framed structure during a fire scene simulation, as well as the temperate distribution and deformation calculation of the structure [15]. Jurickova (2014) pointed out that the geometry, ventilation, and construction method are critical when designing buildings, especially for coordination between civil and fire protection systems in large buildings [16]. Setting an optimal safe distance between buildings is also important for fire protection [17]. Previous studies have achieved good results in different scenarios, although three-dimensional information is still lacking. To solve this problem, building information modeling (BIM) was gradually introduced into simulation modeling [18]. Song et al. (2019) proposed a combinatorial spatial data model (CSDM) to describe the complex geographic relationship with the indoor spatial environment during fires [19]. Machine learning is also widely used to predict the spatial distributions of fire conditions [20]. These studies simulated fire scenarios while considering different complicated factors efficiently and intelligently.

Regarding evacuations in fire events, this involves a reasoning and evaluation process of evacuation response behavior. This could be modeled based on risk prediction and comprehensive evaluations of evacuation conditions during building fire scenario development [21,22]. To decrease the casualties in fire disasters and improve evacuation efficiency, it is vitally important to explore and reveal the factors that impact evacuation [23]. During fire evacuation, human behavior and capability can be significantly influenced by the environmental conditions [24,25], mainly due to temperature, smoke, reduced visibility, and toxic combustion gases [3,22,26]. In addition, several factors influence residents' emergency preparedness, such as fire risk perception, owner or renter status, and building-level emergency preparedness [27]. Building fires pose significant threats to residents, first responders, and the structural system. It is thus beneficial to establish the critical parameters of the building, such as the number of stories, the width of the egress paths, the locations and number of exits, and the locations and number of firefighting device [28,29]. The time interval from the moment of detection of the fire to the moment of final completion of the evacuation to the safety zone must be sufficient. This time condition is generally recognized [30,31]. The capabilities of building fire evacuation modes are evaluated using five main core components, namely the pre-evacuation time, movement and navigation, exit usage, route availability, and flow constraints [32]. In the modeling process, mobile fire evacuation systems and wireless data transmission systems can be dynamically monitored to control the facilities [29,33,34], while indoor navigation technology can be used to obtain or supply spatial–temporal location and navigation information [35]. At the same time, path searching can be gradually explored using a 3D GIS [24], cellular automata (CA) [36], artificial intelligence (AI) [35,37], graph theory [38], or operations research (OR) [31] approaches.

From the above review we can see that there is still a lack of a method for selecting the fire source locations for existing building evacuation plans [39], while influencing factors should be considered for evacuation simulations as much as possible [23]. At the same time, the data related to fire simulations and evacuations are increasing rapidly. Therefore, it is unfortunately difficult to use complicated calculations for personnel evacuation planning, as this requires too many resources [40]. These factors will affect the efficiency of the fire prevention and protection planning process.

In this study, we aim to simplify fire simulation modeling and evacuation path planning. The objectives of this study are: (1) to analyze the spatial and temporal influential factors of building fires based on the realistic worst case; (2) to select fire scenario zones and parameter settings for the simulations; and (3) to design life safety guarantee routes based on a search algorithm.

2. Materials and Methods

The basic idea of the proposed method in this study is to simulate the environmental factors during fire scenarios and thus obtain an evacuation plan. Taking advantage of GIS technology in spatial analysis, a BIM-based building model is applied to the GIS. Outer and internal environmental factors will be simulated by solar radiation and airflow simulation, respectively. After that, different simulation results in different seasons are then analyzed and used for evacuation planning. The fire scenario is then constructed based on the principle of the realistic worst case. A spatial route planning algorithm in GIS, the ant colony algorithm (ACO), is finally used for the evacuation route planning task according to the fire scenario. The overall workflow is illustrated in Figure 1.

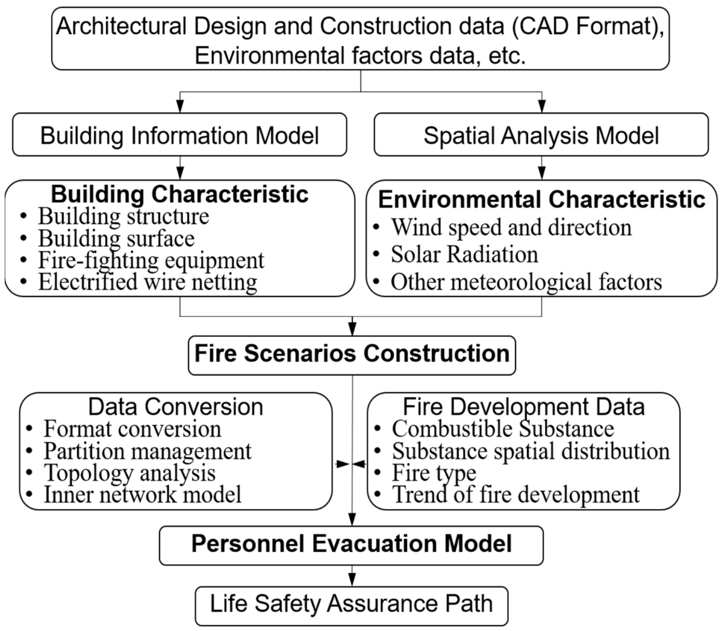

Figure 1. Overall workflow.

2.1. BIM Model Generation

The BIM model is firstly generated from original architectural design and construction files in a CAD format. In order to realize the conversion from the BIM model into GIS data, this study carried on secondary development based on Revit and Visual Studio 2014 platform. The conversion procedure mainly consists of several functions, such as structure transformation, spraying system transformation, pipeline transformation and so on. The transformation procedure mainly has two steps. Firstly, building constructs that require data transformation should be identified from the linked CAD drawing bits. Secondly, the identified building constructs further generate the corresponding 3D entities of Revit. The generated information can be transferred by the external .xml file. In the identification procedure, the function in the CAD secondary development kit was called to extract information from original .dwg files. This function can be encapsulated and invoked in Revit.

2.2. Fire Scenario Construction Based on the Pricipline of the Realistic Worst Case (RWC)

The scenario approach has been successfully used in environmental risk assessments of pesticides [41], and here is introduced into this study for a comprehensive assessment of building fires. A scenario is a synthetic description of an event or series of actions and events, and this approach is widely used by organizations to understand different ways that future events might unfold or to test strategies against uncertain future developments [41]. Scenarios are also only applied to local situations or to a limited number of 'representative' scenarios [42]. In this study, the representative fire scenarios were selected based on serval fire factors.

In general, a fire will occur under specific realistic conditions affected by many factors comprehensively. In realistic conditions, a fire hazard is mainly affected by the basic features, the appendages, and the environmental characteristics of buildings. The level of fire hazard will thus be relatively low if the values of these factors are lower than the risk thresholds according to official standards or laws for fire protection. In order to predict the worst situation, the specific condition with factors closest to the risk thresholds can be seen as the realistic worst case. In several studies the percentile value of factors was used to evaluate the risk of different factors [43–45]. In order to quantitatively reflect the spatial level features of fire factors the study carried on a flow chart of data processing that contains several processes, such as spatial interpolation and simulation, threshold segmentation, and spatial overlay analysis. For example, the spatial characteristics of buildings and environmental factors were overlaid and intersected; the processed result can be expressed in different levels on the spatial scale [46]. Then, the zone of the realistic worst case can be selected according to the related standards. Additionally, this result can then be further used as a fire scenario for personnel evacuation. The environmental factors that make up the realistic worst case can be combined to evaluate fire risks from the spatial and temporal scales. With the calculation of percentiles based on the characteristics of environmental factors, the scenarios with a high fire incidence can be selected as priority zones for fire monitoring and prevention; that is to say, if the scenarios are within the safety standards, the level of fire risk is very low and the building can be regarded as being in a safely protected state. According to the principle of the realistic worst case, the characteristics of the most unfavorable factors possible were selected. Effective factors that are most likely to cause a fire in a real situation were first selected. The worst case does not represent the extreme worst conditions, but instead represents relatively bad effective factors that are likely in reality.

In general, fire scenarios contain a group of effective parameters and factors that need to be inputted into the model, such as the building structure, building surfaces, and micro-metrological factors of the interior and outdoor. The spatial–temporal behaviors of hazard factors were simulated and the damage that was caused by the fire was evaluated. The simulated result was much closer to reality based on the fire scenarios. Therefore, fire scenarios in the fire simulation model will not be overly conservative and the simulation results will not show excessive distortion.

Based on the fire protection standards and codes, such as the Technical Specification for Building Smoke Control and Exhaust Systems GB51251-2017 and the SFPE Handbook of Fire Protection Engineering, the parameter values of fire occurrence can be confirmed. If the fire hazard safety problem is within the prescribed safety standards, it can be considered that a fire will not occur or will not do much harm to the building or residents. On the basis of the realistic worst case, a fire is close to breaking out when the vulnerability and sensitivity of the effective factors accumulate under all possible situations on the whole. The accumulation can be described as a percentile according to the principles of spatial statistics. In this study, fire scenarios were built according to the characteristics of solar radiation, the speed and direction of the wind, the building surfaces, the distribution and types of combustible substances, the operational status of the smoke exhaust system, and the firepower and growth trends. Here, meteorological data were acquired from the National Meteorological Science Data Center (NMSDC, http://data.cma.cn, accessed on 1 December 2021), while building information and other relevant data were obtained from the relevant construction and management departments. By using a building information model (BIM) and geographical information system (GIS), the parameters of effective factors were spatially expressed and simulated across four seasons. When confirming the values of these parameters the percentile values were calculated with every parameter for building fire scenarios, such as the 90th percentile. All simulation results were overlaid and overlapping zones were extracted and classified with several further levels. This could be done by using the spatial overlaying function in ArcGIS software. Through this comprehensive analysis, fire scenarios were selected in different seasons and the parameters of fire scenarios were obtained as inputs for the fire simulation model, allowing consistent and reproducible calculations.

2.2.1. Influencing Factors of Fire Occurrence

Building fires are caused by multiple complicating factors, such as the building structure and surfaces, electric and other networks, indoor and outdoor environmental elements, and human behavior. On the whole, the formative factors of fire can be divided into four categories:

(1) Basic features of the building architecture and its appendages. This category includes the fire load, building material, firefighting equipment, fire compartment, electric equipment and network, smoke control, and exhaust facilities. The complexity of the building and essential facilities greatly affects the path and efficiency of the fire spread. The changes in temperature can be influenced by the thermal conductivity of the building structure. There can also be obvious differences in the degree of smoke obstruction based on the building structure. Fire prevention and control are greatly influenced by the fire prevention facilities and ventilation system. When a building goes into service, basic features of its architecture and appendages need to be checked, accepted, and monitored in the long term.

(2) Environmental factors. All of the environmental factors and local micrometeorological factors play important roles in building fires. Solar radiation can affect the temperature of the building's surfaces, which increase when solar radiation is relatively high and then continue rising. Changes in airflow indoors and outdoors will also be affected by wind speed, causing variations in oxygen concentration in the fire zone. In most cases, the airflow can vary the direction and speed of the fire spread, especially in high winds and dry weather. Additionally, the meteorological factors show significant variations across the four seasons. In general, the frequency of fires is much higher in the spring and autumn.

(3) Fire characteristics. Being affected by combustible substances, fires can present different characteristics, such as in their spread speed, growth trends, destructive effects, and chain reactions. At the same time, fires can present different characteristics according to the growth stage. The effective factors will play different roles at different stages. With the development of fire behavior, the flames will also show different shapes, colors, heights, and temperatures for diverse building materials and structures.

(4) Human behavior. Personnel daily performance is an important factor in monitoring and preventing fire. Human behavior not only refers to the age distribution, fire protection consciousness, and response time, but also to daily management and treatment measures, which are inextricably linked to fire protection behavior. The normal and safe utilization of buildings and related equipment can effectively avoid the occurrence of fire.

According to the classification above, the structures, surfaces, and relevant networks are relatively fixed when a building is in normal use and serviced sufficiently. However, with long-term use these factors will affect the building fire risk with increasing age, although daily management and treatment can enhance the fire protection and prevention ability. Regarding the occurrence and development of fire, these aspects are closely related to the building characteristics and environmental factors. Therefore, ongoing changes in environmental factors will play an important role in fire risk at any time, which is the purpose of this study on fire scenarios.

2.2.2. Influencing Factors of Human Evacuation

It is known that the study of hazard factors of building fires can be effectively used to support the personnel evacuation planning process. The goal of an evacuation in a fire event is to evacuate all personnel safely out of the building before the fire hazard factor poses a risk to their lives. In this paper, we evaluated the safety of the fire environment according to the fire hazards and evacuation time. The evacuation time needs to consider the required safety egress time (RSET) and the available safety egress time (ASET) during a fire. In general, the evacuation criteria should state that the available safety egress time should be no less than the require safety egress time (ASET $\geq$ RSET). If the simulation result is fit to the criteria, the design and construction of the building should meet the fire safety requirements. Otherwise, the building should be optimized to meet the fire safety requirements. Regarding the process of personnel evacuation, relevant fire products and personnel behavior will influence the evacuation time. Several important factors are listed below, all of which will be input into the network model to analyze the personnel evacuation process.

(1) Temperature

After a fire breaks out in a building, the temperature will increase gradually as the fire field heats up. This will lead to serious injuries and risks to personal safety, such as skin and respiratory tract injuries. The National Fire Protection Association (NFPA) has analyzed a mass of data on accidents as well as experiments and has summarized the survival times of the human body under different temperatures (Table 1). According to Table 1, when the temperature of the fire field is no more than 60 °C, human health will not be greatly impacted. People can stay on-site for a short time and have the ability to escape. Human health will be threatened significantly with further temperature increases, even losing the ability to escape.

Table 1. Survival times that the human body can withstand at different temperatures.

Temperature (°C)	Endurable Time (Min)	Temperature (°C)	Endurable Time (Min)
<60	>30	140	4
100	12	160	2
120	7	180	1

(2) Visibility

During the evacuation process, visibility represents the maximum distance at which a person can distinguish an object or direction in smoke. After a fire breaks out in a building, combustible substances burn violently. The large amount of smoke produced will spread gradually, and its concentration will increase. The visibility of emergency personnel will decrease significantly. Therefore, this reduced visibility will seriously affect the evacuation personnel's judgment of the environment inside the building. It will be difficult for people to move towards the correct exit in time, as valuable escape time is likely wasted. It is believed that a visibility of no more than 13 m is needed to satisfy the requirements for personnel escape in the SFPE Handbook of Fire Protection Engineering. In other countries there will be different standards and understandings depending on the different spatial scales. Overall, visibility is an important influencing factor for evacuation in building fires.

(3) Toxic gas

Toxic gas is a major reason for casualties in many situations. The huge amount of smoke can cause personnel suffocation and even death. Additionally, toxic components can cause direct poisoning of the human body. In particular, when carbon monoxide enters the body it will prevent hemoglobin from binding, meaning people will become hypoxic, causing dizziness, nausea, limb weakness, and blurred vision. According to

Table 2, a concentration of carbon monoxide of 500 ppm is a critical value. When the concentration of carbon monoxide is greater than 500 ppm it is difficult to escape, and people show significant adverse reactions. Additionally, smoke particles and suspended particles produced by burning combustible substances produce toxicity and shading, which will have noticeable effects during personnel evacuation (Table 3).

Table 2. Effects on the human body under different CO concentrations.

Concentration of Carbon Monoxide (ppm)	Degree of Injury to Human Body
50	Exposure time should not exceed 8 h
200	Headaches occur between 2 and 3 h
500	No significant effect on human body in one hour
1000	Headache and emesis in 1 h, endangered
3000	Headache and emesis in 15 min, no sensation after 30 min of exposure, endangered
5000	A strong feeling of dizziness, risk of death in 20 min
10,000	Headache and loss of consciousness in 1–2 min, risk of death in 5 min

Table 3. Temperature and CO thresholds during the evacuation path.

Safety Level	Temperature (°C)	CO Volume Fraction $\times 10^6$	Travel Ability
Safety	<42	<50	Passing
Exist risk	42–50	50–200	Passing
Risk	>50	>200	No passing

(4) Evacuation speed

The speed of personnel excavation plays a decisive role in the available safety egress time. The personnel walking speeds in different circumstances were delineated in the SFPE Handbook of Fire Protection Engineering. According to the handbook, walking speeds have been set for different spaces of a building. Personnel speed in clear and spacious zones is 1.1 m/s, while the speed is 0.7 m/s in passageways between seats and bookcases. At the same time, the speed is 0.4 m/s when navigating corners.

2.3. Fire Simulation and Evacuation Planning Based on the Ant Colony Algorithm (ACO)

(1) Fire growth model

The use of a fire growth model is a way of describing the development of a fire. The majority of fires, with the exception of an explosive ignition source, are characterized by a slow progress from the initial stage to a later stage of intense burning. Such fires can be described by the t^2 fire model, as follows:

$$Q_f = at^2 \tag{1}$$

where Q_f represents the rate of heat release from the ignition source, a represents the fire increase modulus, and t represents the ignition time. Based on the fire model, the development stage of the fire can be divided into the initial stage, growth stage, all-round development stage, and spread stage (Table 4). According to the characteristics of the library and combustible substances studied here, the type of fire growth can be thought of as fast, while the fire increase modulus can be set to 0.0469 kw/s^2 in the fire model.

Table 4. Characteristics of four fire growth models according to the t^2 fire model.

Fire Type	Fire Increase Modulus (kw/s^2)	Duration to Q = 1 MW (s)	Combustible Substances
Low speed	0.00293	600	Cleats and plates
Medium speed	0.01172	300	Non-cotton materials
Fast speed	0.04689	150	Foamed plastic and stack board
Enhanced speed	0.18750	75	Formaldehyde material

The scale of the fire depends on the heat release rate. The higher the rate of fire heat release, the greater the danger from the fire. In general, buildings with different characteristics have different heat release rates from the fire source. Therefore, it is important to select a feasible fire heat release rate in the simulation that accounts for most real fire situations, which will mean the simulation results have value. The heat release rates for all kinds of building were delineated in the Technical Specification for Building Smoke Control and Exhaust System GB51251-2017 (Table 5). In this study, the library is an atrium structure without sprinklers. Combined with the realistic worst case, the maximum heat release rate is set as 4 MW in the fire simulation model in this paper.

Table 5. Maximum heat release rates of a fire source in different public places.

Public Places	Maximum Heat Release Rate
Atrium with sprinklers	1.0
Bus garage with sprinklers	1.5
Office or guest room with sprinklers	1.5
Public places with sprinklers	2.5
Shopping mall with sprinklers	3.0
Bus garage with sprinklers	3.0
Supermarket or warehouse with sprinklers	4.0
Atrium without sprinklers	4.0
Office or guest room without sprinklers	6.0
Public places without sprinklers	8.0
Supermarket or warehouse without sprinklers	20.0

(2) Resident evacuation model

The time of the shortest path (TSP) and distance of the shortest path (DSP) are common path-searching strategies. The TSP focuses on minimizing the time of personnel evacuation, while the DSP focuses on personnel evacuation over the lowest path length [47]. Both of these ignore the influence of path conditions on personnel evacuation and cannot satisfy the personnel evacuation requirements in burning buildings. Therefore, the life safety assurance path (LSAP) approach was put forward in this study based on the network model. According to the need for personnel evacuation, the LSAP takes full account of the effects of temperature, smoke, and carbon monoxide, and also effectively avoids fire combustion products. Additionally, it searches the path, striking a balance between the TSP and DSP in order to ensure life safety. In the network model, attribute information for the inner path and fire scenario are input into a spatial database. Attribute information for the inner path can be divided into the path node, path width, and path length. The fire scenario information mainly contains data relating to the wind direction, wind speed, environmental temperature, firepower, fire increase modulus, and sprinkler as well as exhaust facilities. In addition, the path node information includes barriers, turns, intersections, and junctions. Based on the spatial, graphical, and attribute information for the inner path, the network modeling was carried out with topology processing; we then further implemented a network analysis with a path search algorithm.

The indoor network model is different from the outdoor network model, as it is a three-dimensional network model [48,49]. The path in the model has both horizontal and vertical extensions. The network database for the library was adopted using the concept of partition management and divided into different parts according to the number of floors; that is to say, every floor itself contained a separate network model, which can be connected to show safe passageways. Therefore, a large network model was built for the library based on the different parts.

An ant colony search algorithm was then used to analyze the personnel evacuation path, which could be done using the Network Analyst tool in ArcGIS software. The ACO is a simulation algorithm for searching the path of an ant colony when searching for food [50]. Based on rules such as pheromone concentration, it determines the random advance route of an ant colony searching for food from the starting point to the target point. Given the starting point of the path search is i, the target point is j, and the operation expression of the random advance probability can be presented as follows [50]:

$$q_{ij}^{l}(t) = \begin{cases} \frac{\tau_{ij}^{\varphi}(t)\mu_{ij}^{\phi}(t)}{\sum_{s \in allowed_l} \tau_{is}^{\varphi}(t)\mu_{ij}^{\phi}(t)}, j \in allowed_l \\ 0, otherwise \end{cases}. \quad (2)$$

In Equation (2), an individual searching for an exit is denoted by l, and the time consumed is expressed in terms of t. Expectation and pheromone heuristic factors were expressed as ϕ and φ separately. At a given time, t, the probability of a person walking from i to j is denoted by $q_{ij}^{l}(t)$, and the pheromone concentration can be expressed as $\tau_{ij}(t)$. A set of path nodes that an individual, l, can move toward can be expressed as $allowed_l$, and $allowed_l = \{1, 2, \cdots, m-1\} - tab_l$. tab_l represents the node set that has passed by. The heuristic information function corresponding to the section is represented by $\mu_{ij}(t)$. In addition, it is necessary to update pheromones on all paths involved in m target nodes after everyone has gone through a path search cycle. The pheromone transformation is expressed as follows:

$$\tau_{ij}(t+1) = (1-\delta) \times \tau_{ij}(t) + \sum_{t=1}^{n} \Delta\tau_{ij}^{l}(t) \quad (3)$$

In Equation (3), as the time changes, pheromone volatility can be expressed as δ, and $\delta \in (0, 1)$. The number of individuals is denoted as n, and the amount of information released by an individual, l, to path ij in the loop is denoted by $\Delta\tau_{ij}^{l}(t)$.

From Equations (2) and (3) we can see that the ACO is a probabilistic algorithm to find optimal paths. It contains a group of non-intelligent or slightly intelligent agents that show intelligent behaviors by cooperating with each other, thereby providing the possibility of solving complex problems. In this work, the path situations change from moment to moment according to the fire development trend. Therefore, the evacuation path is a topological arithmetic path that is dynamically based on time intervals in the model and supply service.

2.4. Study Area and Data

In this study, the library of the Nanjing Forestry University was selected as the research object. Compared to other buildings, the inner structure of the library is relative complex, the population density is much higher, and the types of combustible substances are very dense. The library adopted a transverse frame structure, which contains the main building and annex building, and its service life is 50 years (Figure 2). The total construction area and base area equal 47230.8 m^2 and 7651.4 m^2, respectively. The building height is 34.9 m, which includes seven floors aboveground and one floor underground. The fire resistance rating is first-class. The earthquake fortification rating is seven degrees. The waterproof grade is first-class. For the inside of the building, the middle of the first and second floors contains an atrium structure, with a rectangle structure from the third floor to the seventh floor. There is a large number of reading rooms and lecture theatres, in addition to a large quantity of books, bookshelves, tables, and chairs in the corridors. Additionally, there are multiple staircases between the floors, distributed in the middle of the four corners of each floor. Therefore, the research object is a typical public agglomeration and key fire monitoring area, for which it is necessary to carry out a fire simulation.

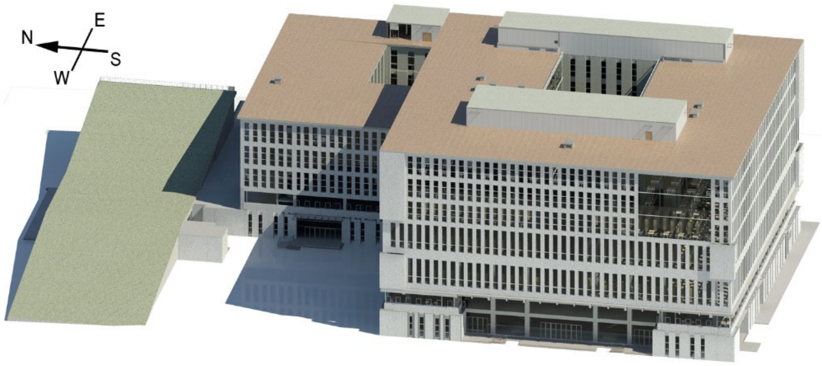

Figure 2. Building information model for the library at the Nanjing Forestry University.

3. Results

3.1. Fire Scenario Construction Results

In this study, the building characteristics were fixed in the simulation model. The fire development trend described with the fire growth model was mainly affected by the fire scenario. Furthermore, the fire scenario was mainly constructed according to environmental elements. Therefore, the solar radiation and wind were selected based on the realistic worst case. Spatial and temporal analyses of these aspects can be seen below.

3.1.1. Spatial and Temporal Analyses of Solar Radiation

By using the solar radiation model in ArcGIS software, an illumination analysis in the library was processed with an illumination and solar radiation equation time range of 08:00 to 18:00. The spatial solar radiation was simulated in four seasons around the library. Due to the effects of occlusion, the solar radiation centered on the building gradually reduced in the library and the surrounding area (Figure 3). Additionally, the solar radiation presented an increasing trend in the first half of year and reduced in the second half of the year. Across the four seasons, solar radiation reached its maximum in summer at 4500 w/m^2 and declined to its minimum in winter at 2080 w/m^2. Compared with the value of 4020 w/m^2 in autumn, the maximum solar radiation was much lower in spring at 3240 w/m^2. According to mathematical–statistical results and the RWC, the 90th percentile value was nearly the maximum over the four seasons. Therefore, the maximum value was selected for the construction of fire scenarios in different seasons.

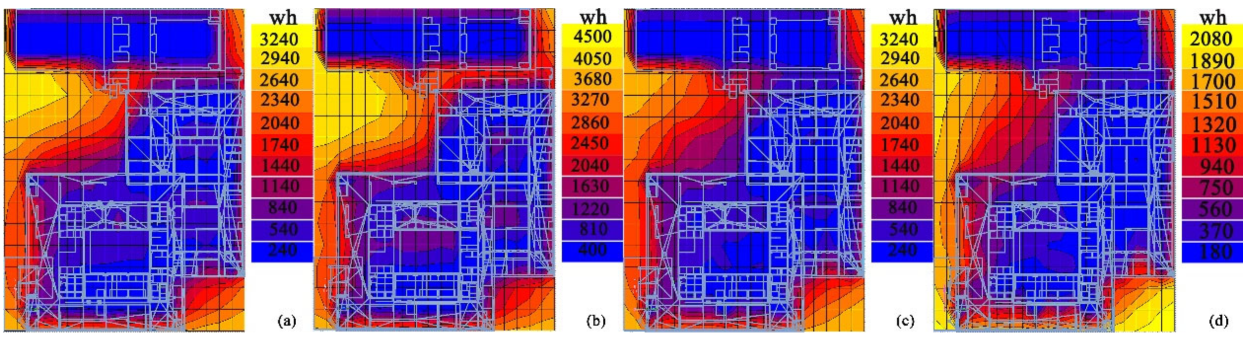

Figure 3. Spatial distribution of solar radiation in spring (**a**), summer (**b**), autumn (**c**), and winter (**d**).

3.1.2. Spatial and Temporal Analyses of Outside Temperature and Wind

Spatial and temporal changes in temperature and wind were simulated across the four seasons using ArcGIS software. Influenced by the monsoon climate, the seasonal characteristics showed obvious differences in the study field (Figure 4 and Table 6). First, the temperatures presented vast differences in different seasons, with the mean maximum temperatures being 19.7 °C, 30.7 °C, 21.8 °C, and 8.6 °C across the four seasons. The variations in inner temperature kept a close relationship with the outdoor temperature.

Secondly, according to the spatial and temporal simulation results, the wind direction was mainly southeasterly in summer as well as autumn and northeasterly in winter as well as spring. The mean maximum wind speed reached 4.4 m/s in spring, 6 m/s in summer, 4.7 m/s in autumn, and 5 m/s in winter. Additionally, the duration in the main wind direction lasted for 62.5%, 70.1%, 50.2%, and 73.4% across spring, summer, autumn, and winter, respectively. There were occasional easterly and northerly winds. Therefore, fire at different speeds can spread to the northwest in summer as well as autumn and to the southeast in winter as well as spring.

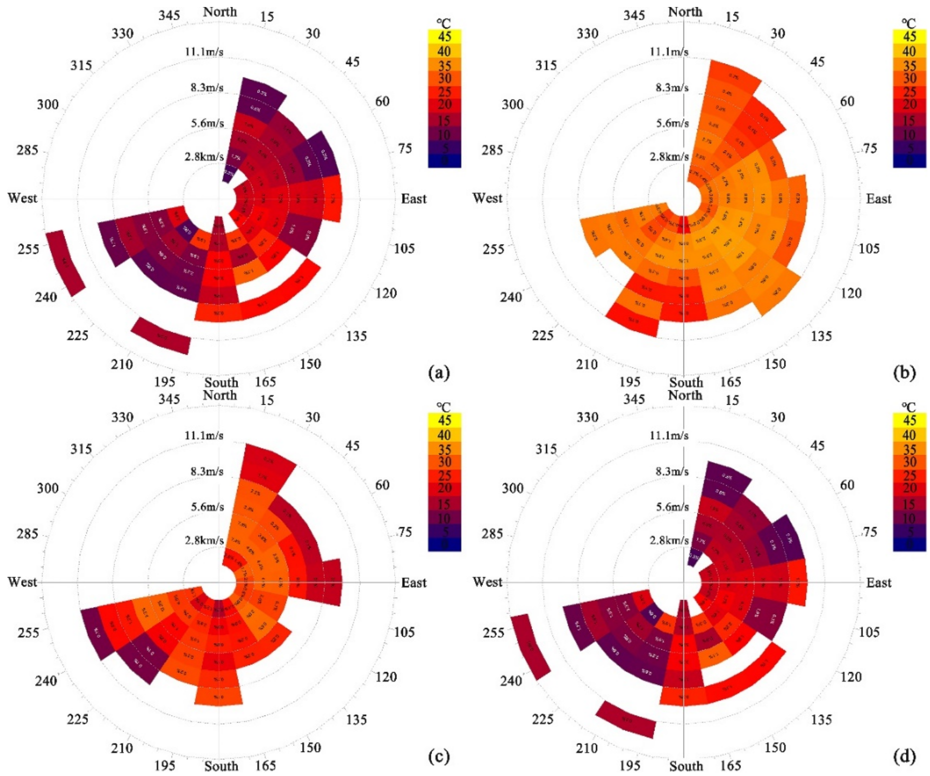

Figure 4. Temporal variations in wind frequency and temperature around the library in spring (**a**), summer (**b**), autumn (**c**), and winter (**d**).

Table 6. Characteristics of temperature and wind around the library across the four seasons.

Meteorological Factors	Spring	Summer	Autumn	Winter
Mean maximum temperature (°C)	19.7	30.7	21.8	8.6
Mean maximum wind speed (m/s)	4.4	6	4.7	5
Mainly wind direction	Northwest	Southeast	Southeast	Northwest

3.1.3. Spatial and Temporal Analyses of Inside Wind

According to the spatial and temporal simulations of outside wind presented above, the inner wind and airflow over the four seasons were further analyzed using Ecotect software in this study (Figure 5). The acquisition of internal parameters requires the simulation results of outdoor environmental parameters, such as the environmental parameters of the starting position of the passage or entrance. The library was mainly affected by northwesterly and southeasterly winds. Therefore, the direction, speed, and strength of the inner wind will also change correspondingly, showing vast spatial and temporal differences. The details regarding the analysis of the inner wind and airflow are presented below.

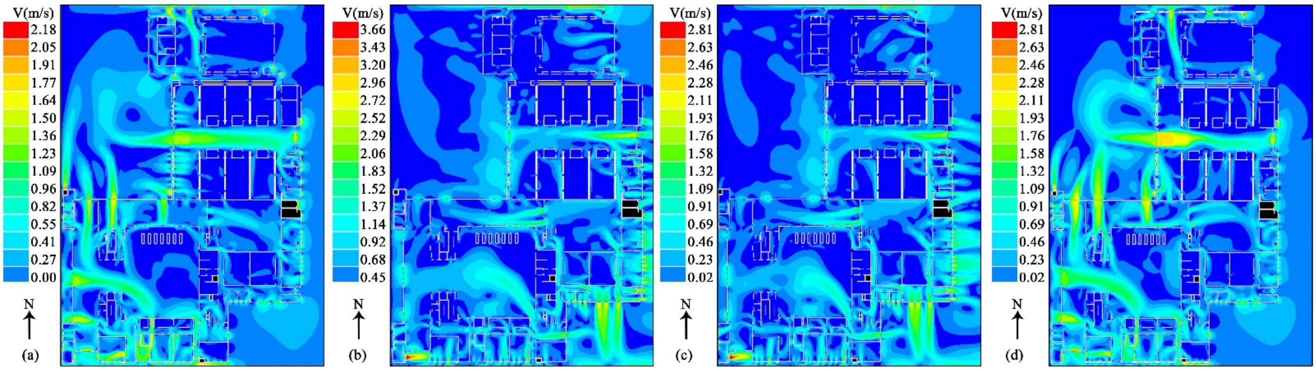

Figure 5. Spatial variation characteristics of inner wind over four seasons, in spring (**a**), summer (**b**), autumn (**c**), and winter (**d**).

First, influenced by northwesterly winds with a maximum of 4.4 m/s in spring, airflow moves from east to west along the corridor (Figure 5a). For the annex building, the airflow cannot result in a baffling effect because there are fewer obstacles in the corridor. When the airflow moves through the corridor in the hall the wind does not weaken. The main building is mainly affected by the airflow coming from the western gate and the northwest side door. After these two airflows meet together in the hall the direction of the airflow will experience a 45° deflection and change to the northwest. Therefore, once a fire breaks out in the northwest zone it will spread indoors under the influence of the airflow.

Second, compared with other seasons, the strength of the southeasterly wind at 6.0 m/s is much more significant in summer, while the speed of the inner airflow is relatively high in the whole library. The main building is more prominently affected by southeasterly wind. As seen in Figure 5b, one airflow can enter the reading room from both the south as well as the east and move along the corridor, reaching the atrium at high speed. Additionally, another airflow travels through the corridor channel located on the north zone from east to west in the main building. According to the spatial distribution of the airflow, the first airflow coming from the reading room moves quickly and its effective area is much larger. If a fire breaks out here, the fire and smoke will spread to other zones quickly and could even affect the safety of the whole library.

Third, the wind speed goes down to some extent in autumn, although the spatial distribution and movement of the airflow are similar to summer. The southeast zone is still significantly affected by the airflow, although the local strength is reduced (Figure 5c). In autumn the maximum speed of the airflow is 2.8 m/s, although the airflow has relatively low speed in the majority of the area. In this condition, smoke can gather easily, which will lead to high concentrations. Additionally, fire spreads with the movement of airflow. Therefore, the southeast zone is secure and safe.

Lastly, two airflows travel from the main door on the west and the side door on the northwest in the winter. These zones are obviously affected by the northwest wind at 4.7 m/s. The speed of the airflows can reach 2.5 m/s in some local zones. When the two airflows meet together in the hall their directions will be deflected. Lastly, the airflow will move to the reading room on the southeast of the main building. In addition, another airflow passes through the northern corridor from west to east. For the annex building, the central corridor is obviously affected by the airflow, especially the door on the west side. The speed of the airflow reaches 2.5 m/s and gradually reduces when it goes through the central corridor. On the whole, the northwest zone is an important area to monitor in the main building; smoke and fire can spread quickly here and can further affect the whole building.

3.1.4. The Construction of Fire Scenarios in the Four Seasons

According to the principles of the realistic worst case, the location of a fire scenario is selected mainly based on the most likely location for a fire, the level of fire threat to personnel, and the speed of fire development. Here, there are several factors that need to be considered across the four seasons, such as extreme solar radiation, the direction of the inner airflow, the spatial distribution of combustible substances, and the sprinkler and fire protection system. With comprehensive consideration, the above factors can be processed using a spatial overlay analysis (Figure 6) for the different floors. There are four zones with high solar radiation, obvious airflow, and high concentrations of combustible substance, which were selected as fire scenario zones for the four seasons. Hence, the characteristic parameters of the fire scenario zones are confirmed (Table 7).

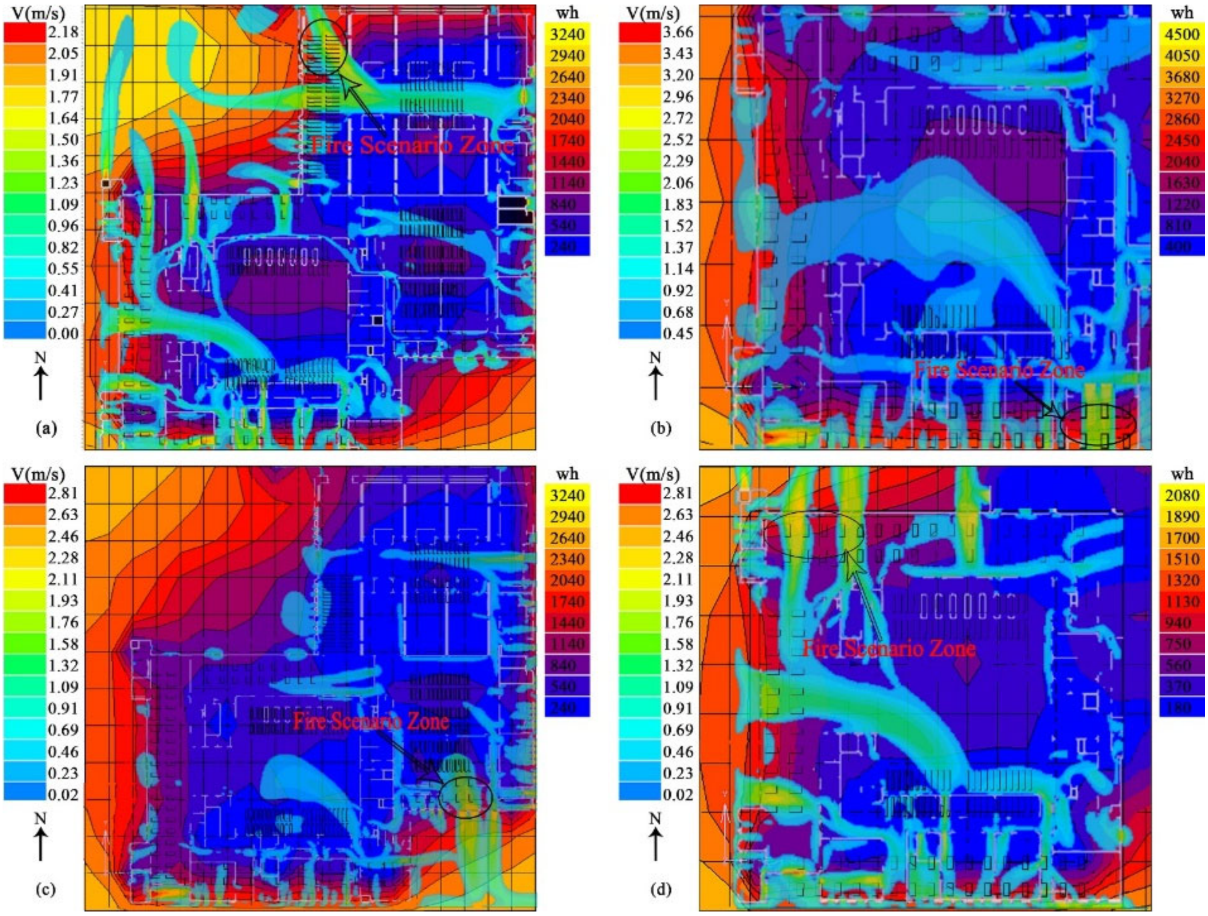

Figure 6. Results for the fire scenario zones across the four seasons in spring (**a**), summer (**b**), autumn (**c**), and winter (**d**).

Table 7. Characteristic parameters of the fire scenario zones across the four seasons.

Location	Season	Wind Direction	Wind Speed (m/s)	Solar Radiation (w/m^2)	Temperature (°C)	Firepower (mw)	Fire Increase Modulus (kw/s^2)
Bookcase in northwest corner on the third floor	Spring	Northwesterly	4.4	3240	19.7	4	0.0469
Reading room in southeast corner on the sixth floor	Summer	Southeasterly	6.0	4500	30.7	4	0.0469
Reading room in southeast corner on the second floor	Autumn	Southeasterly	4.7	3240	21.8	4	0.0469
Bookcase in northwest corner on the sixth floor	Winter	Northwesterly	5.0	2080	8.6	4	0.0469

According to the principles of the realistic worst case, representative fire scenarios were selected based on the spatial overlay analysis of the wind speed, solar radiation, temperature, firepower, and fire increase modulus in the library. The characteristic parameters of the fire scenario zones showed differences across the four seasons. In spring, the fire scenario zone was on the third floor in the northwest of the annex building (Figure 6a). This zone is obviously affected by northeasterly wind at a speed of 4.4 m/s. The solar radiation is 3240 w/m^2, which is much higher than in the other areas. There are many bookcases and books arranged here. Therefore, the zone is likely to be upstream of the fire. In summer, the fire scenario zone was on the sixth floor in the southeast of the main building (Figure 6b). Influenced by high solar radiation, temperature, and wind speed, the zone is also relatively dangerous. In autumn, after comprehensive consideration of the different factors, the fire scenario zone was selected as being on the second floor in the southeast of the annex building (Figure 6c). In winter, with the overlay analysis of raster data for different factors, the fire scenario zone was selected as being on the sixth floor in the northwest of the main building (Figure 6d). On the whole, the selection of fire scenario zones took into account the risks of several factors, such as wind speed, wind direction, solar radiation, temperature, firepower, fire increase modulus, and sprinkler and fire protection systems. The parameters of the fire scenario can be directly put into a fire simulation and personnel evacuation model for the effective daily prevention and monitoring of fire in the key areas.

3.2. Analysis of Available Evacuation Times for Different Safe Passageways

In order to analyze the available evacuation times for different safe passageways we numbered all such passageways (Figure 7). Combined with the tolerance of the human body to fire products, the development trend and law of combustion products were simulated and predicted for the different floors and evacuation passageways in the building, involving carbonic oxide, smoke, and temperature. The times taken to reach critical values of fire products can be thought as the available evacuation times for different passageways. Additionally, the maximum time for the simulation was set to 900 s in the study. Then, the critical values of fire products were acquired for the key passageways to be used as personnel evacuation exits, which were relatively dangerous (Table 8).

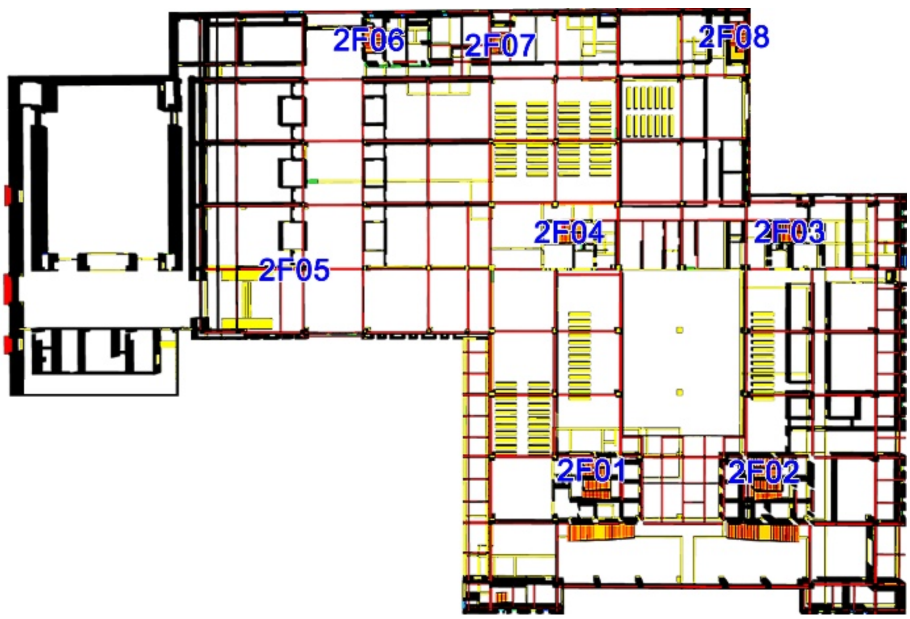

Figure 7. Evacuation passageways on the second floor as an example.

Table 8. Times taken to reach critical values of fire products in evacuation passageways (in seconds).

Season	Location	Visibility	Temperature	CO	Critical Time
Spring	2F06	900	900	366	366
	3F05	90	236	145	90
	3F06	313	900	302	302
	4F05	500	900	520	500
	4F06	252	900	308	252
	4F07	336	900	900	336
	Northern corridor on 2F	900	900	900	900
	Northern corridor on 3F	313	900	302	302
	Eastern corridor on 4F	532	900	513	513
Summer	6F02	242	900	276	242
	6F03	900	153	253	153
	7F02	253	900	352	253
	7F03	900	900	372	372
	Southern corridor on 6F	230	432	163	163
	Southern corridor on 7F	275	900	366	275
Autumn	2F06	259	336	304	259
	2F07	235	900	232	232
	Southeastern zone on 2F	221	254	232	212
Winter	6F01	72	900	249	72
	6F04	239	900	315	239
	7F01	254	900	298	254
	7F04	336	900	412	336
	Northern zone on 6F	405	900	469	405

It is known that personnel safety will be threatened if one of the fire products reaches its critical value. According to the simulation results (Table 8), obvious differences exist in the numbers of relatively unsafe passages across the four seasons during the simulated time period. The times when the fire products reached their critical values are also very different between the different safe passageways. First, the evacuation passageway with the shortest critical time is located at the fifth exit on the third floor in spring, taking only 90 s. The sixth exit on the sixth floor was next, at 252 s. Other passageways are relatively safe in the building. Second, the evacuation passageway with the shortest critical time appears at the third exit on the sixth floor, taking 153 s in summer, followed closely by the southern corridor on the sixth floor at 163 s. Third, the number of relatively unsafe passageways is lowest in autumn; however, the critical time is much closer and shorter. The earliest time that the critical value appears is at 212 s in the southeastern zone on the second floor. Lastly, the critical values for the fire products are reached at the first exit on the sixth floor after only 72 s in winter. The lower floors are much safer in the building. In other words, under the influence of many factors, the temporal and spatial characters of fire products reaching critical values are different over the four seasons, meaning the personnel evacuation results will also differ significantly at various temporal and spatial scales.

4. Discussion

Based on the analysis of the fire scenarios and available evacuation times, the center of the high fire risk zone was selected as the starting point for personnel evacuation in the study. The available evacuation times for key passageways and risk zones were set as point obstacles and surface obstacles. By using the ant colony search algorithm and a spatial overlay analysis on the basis of fire scenario simulation results, people in the high-risk zone can obtain a life safety assurance path with high visibility, low carbon monoxide, good road conditions, and a long available evacuation time (Figure 8).

The LSAP distance is 61.7 m, while the available evacuation time is 86.2 s in spring (Table 9). The path starts from the starting point in the middle aisle on the north side of the third floor and turns east and right along the middle aisle among bookcases to the middle aisle on the east side of the annex building (Figure 7), where people can be evacuated from the seventh-floor stairs. According to the results of the fire simulation at 200 s after a fire broke out, the influence of the fire products only exceeded the standards in the starting section of the LSAP. As the DSP was closed during the fire scenario, the fire products exceeded critical values on most sections of the path, which also occurred in the middle aisle of the TSP. After 400 s, the range of the influence of fire products tended to be stable. The TSP still exceeded the safety risk thresholds. On the contrary, for the LSAP, the seventh-floor stairway was not restricted by fire products. Therefore, it can be seen that the LSAP conditions were fit for personnel evacuation, although the available evacuation time was relatively long.

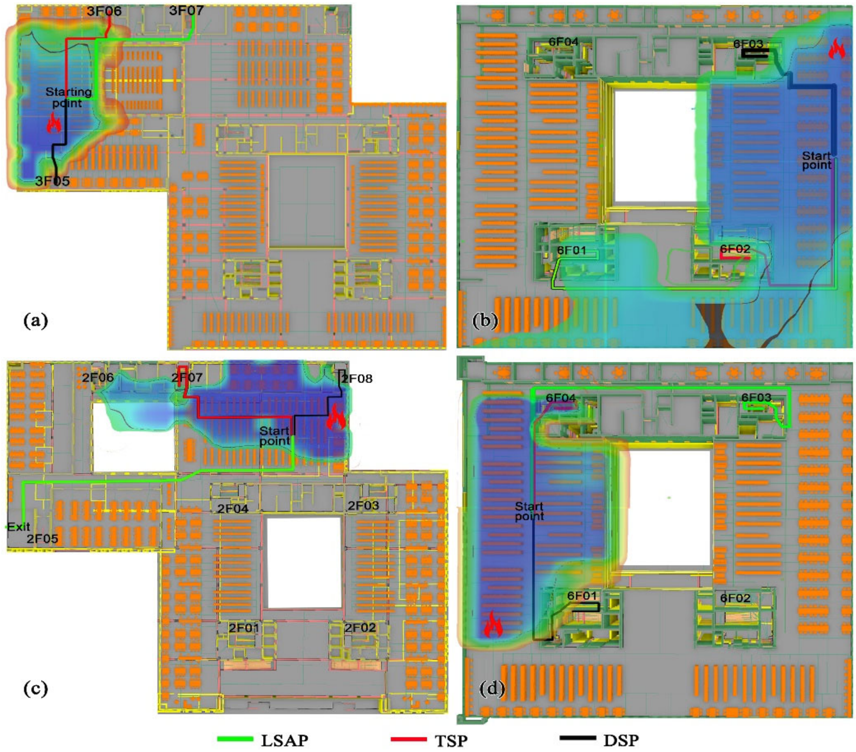

Figure 8. Spatial differences between evacuation passageways across the four seasons: (**a**) spring; (**b**) summer; (**c**) autumn; and (**d**) winter.

Table 9. Comparative analysis of the parameters for different evacuation passageways in spring.

Parameters	TSP	DSP	LSAP
Path length (m)	41.5	49.2	61.7
Path time (s)	74.1	72.6	86.2
Number of path nodes	16	12.0	14.0
Available evacuation time (s)	0.0	302.0	900.0
Limit to critical value of stairway	Yes	Yes	No
Shortest distance to fire scenario (m)	2.1	10.5	10.5

Here, the distance of the life safety assurance path was 94.0 m, and its available evacuation time was 125.3 s in summer (Table 10). The LSAP overlapped with the TSP over the original section (Figure 7). However, with the development of the fire risk, the LSAP to the other floors was much lower than with the TSP. Therefore, we selected the first floor stairway as the exit. About 150 s after the fire started, the section of the LSAP influenced by the fire products was much smaller than the DSP. The section of the life safety route affected by fire was much shorter than for the DSP. After 300 s, the influence of the fire products became stable in the building. The second stairway in the TSP was seriously affected by fire products. The visibility, temperature, and carbon monoxide all exceeded the critical values. In contrast, the fire products in the first stairway in the LSAP did not reach the critical value. These conditions were also suitable for personnel evacuation, although no advantages were seen at all in terms of time or distance.

Table 10. Comparative analysis of the parameters of different evacuation passageways in summer.

Parameters	TSP	DSP	LSAP
Path length (m)	75.2	76.6	94.0
Path time (s)	110.7	110.0	125.3
Number of path nodes	19.0	14.0	15.0
Available evacuation time (s)	0.0	242.0	900.0
Limit to critical value of stairway	Yes	Yes	No
Shortest distance to fire scenario (m)	1.8	11.3	11.3

Here, the distance of the life safety assurance path was 53.6 m, and its available evacuation time was 56.2 s in autumn (Table 11). For the evacuation path and direction, these were far away from the fire scenario (Figure 7). For this path we selected the lateral corridor on the second floor, meaning that people must go through the exit to the exterior on the left side in the annex building. Compared to the DSP and TSP, the LSAP has fewer nodes, meaning that people can avoid twists and turns during the evacuation process. About 100 s after the fire started, the visibility, temperature, and carbon monoxide exceeded the critical values in most sections of the DSP and partial sections of the TSP. After 200 s, the section length of the TSP affected by fire products gradually increased, meaning it was not fit for personnel evacuation. For the LSAP, the extent of fire products affected by southeast airflow spread to the north. Although the visibility in parts of the original section was lower than 10 m, the LSAP was still satisfactory for evacuation.

Table 11. Comparative analysis of the parameters of different evacuation passageways in autumn.

Parameters	TSP	DSP	LSAP
Path length (m)	39.6	41.3	53.6
Path time (s)	53.3	52.7	56.2
Number of path nodes	7.0	6.0	5.0
Available evacuation time (s)	0.0	90.0	900.0
Limit to critical value of stairway	Yes	Yes	Null
Shortest distance to fire scenario (m)	0.0	6.2	5.1

The distance of the life safety assurance path was 93.2 m, and its available evacuation time was 120.7 s in winter (Table 12). The LSAP started at the starting point, followed the middle aisle of bookcases to the east corridor, and reached the third stairway on the sixth floor (Figure 7). According to the simulation results, the LSAP overlapped with the TPS in the path bend. The fourth stairway was obviously influenced by fire products, meaning that the third stairway was selected as the exit. Although the number of turns and the distance gave no advantages, the LSAP conditions were good. About 150 s after the fire started, most sections of the DSP were affected by fire products. The visibility, temperature, and carbon monoxide exceeded the critical values that a person can bear. The conditions for the LSAP and TSP were suitable for evacuation. After 300 s, the fire products seriously affected the fourth stairway, such that it could not be selected as an exit. Therefore, the LSAP was a relatively better path for personnel evacuation.

Table 12. Comparative analysis of the parameters of different evacuation passageways in winter.

Parameters	TSP	DSP	LSAP
Path length (m)	77.8	79.7	93.2
Path time (s)	106.9	106.0	120.7
Number of path nodes	15.0	13.0	16.0
Available evacuation time (s)	0.0	239.0	900.0
Limit to critical value of stairway	Yes	Yes	Null
Shortest distance to fire scenario (m)	2.1	12.6	12.6

In sum, the path selection process should minimize time and distance in consideration of personal safety. Additionally, with the development of spatial information, the Internet of Things, artificial intelligence, and other technologies, fire product and path evacuation simulations will be able to account for indoor positioning and navigation in real time, supplying adaptation measures for fire emergencies and firefighting in very large and tall buildings. The accurate construction of fire scenarios can also further improve the speed of fire emergency responses.

5. Conclusions

According to the principle of the realistic worst case, this study put forward methods and ideas for fire scenario construction as well as a description of the life safety assurance path via the integration of a BIM and GIS. Using a spatial–temporal analysis and an overlay analysis, the effective factors of building fires selected were assessed under fire scenarios. The characteristic parameters of fire scenarios were acquired for the fire simulation model. Based on the developmental trend of fire behavior, an ant colony search algorithm was furtherly used for personnel evacuation planning. The following conclusions can be drawn from the study.

Firstly, along with the fire increase trend, fire heat release rate, and working status of the fire protection and prevention system, the characteristic parameters of the fire scenarios were acquired according to spatial–temporal simulation of environmental factors. These parameters reflect the realistic worst case of fire in the building and can be entered into the fire and personnel evacuation simulation model for the protection and prevention of fire in daily life. A network model was then built based on the path attribute and fire scenario information. The building contained many exit passageways on different floors, and a joint topological analysis was performed for the network model of the whole building. The ant colony search algorithm was then used to assess the life safety assurance path based on the different fire scenarios and the development trends across the four seasons. The availability of the LSAP was compared with the TSP and DSP in terms of the safety, available evacuation time, and path distance. It was found that the LSAP reduced the path distance and consumed time as much as possible, ensuring personnel safe evacuation.

Although this study is a preliminary exploration on the integration of a BIM and GIS into fire scenario construction and evacuation planning, limitations still remain. Firstly, the current work could only be performed on the basis of different software tools as well as multi-source/format data; an integrated framework in an 'all-tools-in-one-package' needs to be further developed. Secondly, evacuation planning results are still on the basis of a 2D plane; the rich 3D information from the original BIM model is not well-used to achieve a real 3D analysis. Future work will mainly focus on introducing 3D information into fire scenario analysis, and corresponding methods are in need of exploration.

Author Contributions: Conceptualization: Qiang Yang; methodology: Qiang Yang and Xu Zhang; software: Zhongren Zhang; writing—original draft preparation: Qiang Yang and Longjiang He; writing—review and editing: Jiaming Na; visualization: Xiaojie Yan; funding acquisition: Qiang Yang and Longjiang He. All authors have read and agreed to the published version of the manuscript.

Funding: This work was financially supported by the National Science Foundation (No. 42101430) and also funded by the State Key Laboratory of Geo-Information Engineering (No. SKLGIE2018-K-4-1).

Institutional Review Board Statement: Not applicable.

Informed Consent Statement: Not applicable.

Data Availability Statement: Data from this research will be available upon request to the authors.

Conflicts of Interest: The authors declare no conflict of interest.

References

1. Yang, J.T.; Yang, Y.; Liang, J. Full-scale experimental and numerical simulation of fire in a High-rise Residential Building. In *Advances in Industrial and Civil Engineering, Pts 1–4*; Wang, L.H., Xu, G., Eds.; Advanced Materials Research; Trans Tech Publications Ltd.: Zurich, Switzerland, 2012; Volume 594–597, pp. 2251–2256.
2. Huang, Y.; Li, H.M.; Chen, C.H. *A Fire Risk Assessment Scheme for Underground Public Building Based on FPN*; Hong Kong Polytechnic Univ: Kowloon, Hong Kong, 2009; pp. 1426–1429.
3. Peacock, R.D.; Averill, J.D.; Reneke, P.A.; Jones, W.W. Characteristics of fire scenarios in which sublethal effects of smoke are important. *Fire Technol.* **2004**, *40*, 127–147. [CrossRef]
4. He, C.Y.; Li, C.Y. Visual analysis of studies on the simulation of fire based on knowledge graph. *Fire Sci. Technol.* **2019**, *38*, 1615–1623.
5. Ralph, B.; Carvel, R. Coupled hybrid modelling in fire safety engineering; a literature review. *Fire Saf. J.* **2018**, *100*, 157–170. [CrossRef]
6. Huang, X.X.; Li, H.G.; Li, X.; Zhang, L. Fire numerical simulation analysis for large-scale public building in 3D GIS. In *Proceedings of the 2019 IEEE International Geoscience and Remote Sensing Symposium—IGARSS 2019, Yokohama, Japan, 28 July–2 August 2019*; IEEE: New York, NY, USA, 2019; pp. 7522–7525.
7. Zhang, G.W.; Zhou, X.; Zhu, G.Q.; Yan, S. A new accident analysis and investigation model for the complex building fire using numerical reconstruction. *Case Stud. Therm. Eng.* **2019**, *14*, 9. [CrossRef]
8. Zhang, J.; Weng, J.W.; Zhou, T.N.; Ouyang, D.X.; Chen, Q.P.; Wei, R.C.; Wang, J. Investigation on Smoke Flow in Stairwells induced by an Adjacent Compartment Fire in High Rise Buildings. *Appl. Sci.* **2019**, *9*, 18. [CrossRef]
9. Ryder, N.L.; Sutula, J.A.; Schemel, C.F.; Hamer, A.J.; Van Brunt, V. Consequence modeling using the fire dynamics simulator. *J. Hazard. Mater.* **2004**, *115*, 149–154. [CrossRef] [PubMed]
10. Wang, Y.C. Performance of steel-concrete composite structures in fire. *Prog. Struct. Eng. Mater.* **2005**, *7*, 86–102. [CrossRef]
11. Nguyen, Q.T.; Tran, P.; Ngo, T.D.; Tran, P.A.; Mendis, P. Experimental and computational investigations on fire resistance of GFRP composite for building facade. *Compos. Pt. B-Eng.* **2014**, *62*, 218–229. [CrossRef]
12. Cheng, H.; Hadjisophocleous, G.V. Dynamic modeling of fire spread in building. *Fire Saf. J.* **2011**, *46*, 211–224. [CrossRef]
13. Xiao, Y.; Ma, J. Fire simulation test and analysis of laminated bamboo frame building. *Constr. Build. Mater.* **2012**, *34*, 257–266. [CrossRef]
14. Goldsworthy, M. Dynamic coupling of the transient system simulation and fire dynamics simulation programs. *J. Build. Perf. Simul.* **2012**, *5*, 105–114. [CrossRef]
15. Bi, R.; Liu, Y.J.; Yan, Y.M.; Yao, L.H. Numerical Analysis of Fire Behavior of Reinforced Concrete Frame Structure. In *Applied Mechanics and Materials I, Pts 1–3*; Li, G., Chen, C., Eds.; Applied Mechanics and Materials; Trans Tech Publications: Bäch, Switzerland, 2013; Volume 275–277, p. 1024.
16. Jurickova, M. Fire dynamic simulation and impact of water sprinkler systems to heat flow. In *Advanced Building Construction and Materials 2013*; Palko, M., Deakova, K., Eds.; Advanced Materials Research; Trans Tech Publications Ltd.: Zurich, Switzerland, 2014; Volume 855, pp. 187–190.
17. Pesic, D.; Zigar, D.; Raos, M.; Anghel, I. Simulation of fire spread between residential buildings regarding safe separation distance. *Teh. Vjesn. Tech. Gaz.* **2017**, *24*, 1137–1145. [CrossRef]
18. Wang, S.H.; Wang, W.C.; Wang, K.C.; Shih, S.Y. Applying building information modeling to support fire safety management. *Autom. Constr.* **2015**, *59*, 158–167. [CrossRef]
19. Song, Y.Q.; Niu, L.; Li, Y. Combinatorial Spatial Data Model for Building Fire Simulation and Analysis. *Isprs Int. J. Geo-Inf.* **2019**, *8*, 408. [CrossRef]
20. Lattimer, B.Y.; Hodges, J.L.; Lattimer, A.M. Using machine learning in physics-based simulation of fire. *Fire Saf. J.* **2020**, *114*, 15. [CrossRef]
21. Dimyadi, J.; Solihin, W.; Amor, R. Using IFC to Support Enclosure Fire Dynamics Simulation. In *Advanced Computing Strategies for Engineering, Pt Ii*; Smith, I.F.C., Domer, B., Eds.; Lecture Notes in Computer Science; Springer International Publishing Ag: Cham, Switzerland, 2018; Volume 10864, pp. 339–360.
22. Tan, L.; Hu, M.Y.; Lin, H. Agent-based simulation of building evacuation: Combining human behavior with predictable spatial accessibility in a fire emergency. *Inf. Sci.* **2015**, *295*, 53–66. [CrossRef]
23. Hu, Y.L.; Wang, X.; Wang, F.Y. A Quantitative Study of Factors Influence on Evacuation in Building Fire Emergencies. *IEEE Trans. Comput. Soc. Syst.* **2018**, *5*, 544–552. [CrossRef]
24. Tang, F.Q.; Ren, A.Z. GIS-based 3D evacuation simulation for indoor fire. *Build. Environ.* **2012**, *49*, 193–202. [CrossRef]
25. Zhu, R.H.; Lin, J.; Becerik-Gerber, B.; Li, N. Human-building-emergency interactions and their impact on emergency response performance: A review of the state of the art. *Saf. Sci.* **2020**, *127*, 19. [CrossRef]
26. Suvar, M.C.; Kovacs, I.; Pasculescu, V.M.; Vlasin, N.I.; Florea, G.D. Analysis of Human Behavior And Evacuation In Building Fires Using Computer Evacuation Models. *Environ. Eng. Manag. J.* **2019**, *18*, 921–928. [CrossRef]
27. Glauberman, G.; Qureshi, K. Exploratory Qualitative Study of Fire Preparedness Among High-rise Building Residents. *PLoS Curr.* **2018**, *10*. [CrossRef]
28. Kodur, V.K.R.; Venkatachari, S.; Naser, M.Z. Egress Parameters Influencing Emergency Evacuation in High-Rise Buildings. *Fire Technol.* **2020**, *56*, 2035–2057. [CrossRef]

29. Jiang, H.X. Mobile Fire Evacuation System for Large Public Buildings Based on Artificial Intelligence and IoT. *IEEE Access* **2019**, *7*, 64101–64109. [CrossRef]
30. Kalmykov, S.P.; Esin, V.M. Fire detection time. *Pozharovzryvobezopasnost* **2017**, *26*, 52–63. [CrossRef]
31. Mirahadi, F.; McCabe, B. EvacuSafe: Building Evacuation Strategy Selection Using Route Risk Index. *J. Comput. Civil. Eng.* **2020**, *34*, 16. [CrossRef]
32. Ronchi, E.; Nilsson, D.; Kuligowski, E.D.; Peacock, R.D.; Reneke, P.A. Assessing the Verification and Validation of Building Fire Evacuation Models. *Fire Technol.* **2016**, *52*, 197–219. [CrossRef]
33. Han, Z.Y.; Weng, W.G.; Zhao, Q.L.; Ma, X.; Liu, Q.Y.; Huang, Q.Y. Investigation on an Integrated Evacuation Route Planning Method Based on Real-Time Data Acquisition for High-Rise Building Fire. *IEEE Trans. Intell. Transp. Syst.* **2013**, *14*, 782–795. [CrossRef]
34. Yan, F.T.; Hu, Y.H.; Jia, J.Y.; Guo, Q.H.; Zhu, H.H.; Pan, Z.G. RFES: A real-time fire evacuation system for Mobile Web3D. *Front. Inf. Technol. Electron. Eng.* **2019**, *20*, 1061–1074. [CrossRef]
35. Deng, H.; Ou, Z.B.; Zhang, G.J.; Deng, Y.C.; Tian, M. BIM and Computer Vision-Based Framework for Fire Emergency Evacuation Considering Local Safety Performance. *Sensors* **2021**, *21*, 3851. [CrossRef]
36. Yang, R.; Jiang, Q.H.; Fang, Z. A fire evacuation model for indoor buildings based on the improved Cellular Automaton. *Disaster Adv.* **2013**, *6*, 19–23.
37. Ran, H.C.; Sun, L.H.; Gao, X.Z. Influences of intelligent evacuation guidance system on crowd evacuation in building fire. *Autom. Constr.* **2014**, *41*, 78–82. [CrossRef]
38. Hu, Y.L.; Liu, X.W. Optimization of Grouping Evacuation Strategy in High-rise Building Fires Based on Graph Theory and Computational Experiments. *IEEE-CAA J. Autom. Sin.* **2018**, *5*, 1104–1112. [CrossRef]
39. Wang, N.; Gao, Y.; Li, C.Y.; Gai, W.M. Integrated agent-based simulation and evacuation risk-assessment model for underground building fire: A case study. *J. Build. Eng.* **2021**, *40*, 13. [CrossRef]
40. Papinigis, V.; Geda, E.; Lukosius, K. Design of people evacuation from rooms and buildings. *J. Civ. Eng. Manag.* **2010**, *16*, 131–139. [CrossRef]
41. Li, W.-J.; Qin, Z.-H.; Zhang, M.-H.; Browde, J. An index method to evaluate growers' pesticide use for identifying on-farm innovations and effective alternative pest management strategies: A case study of winegrape in Madera County, California. *J. Zhejiang Univ. Sci. B* **2011**, *12*, 226–246. [CrossRef]
42. Centofanti, T.; Hollis, J.; Blenkinsop, S.; Fowler, H.; Truckell, I.; Dubus, I.; Reichenberger, S. Development of agro-environmental scenarios to support pesticide risk assessment in Europe. *Sci. Total Environ.* **2008**, *407*, 574–588. [CrossRef]
43. Nolan, B.T.; Dubus, I.G.; Surdyk, N.; Fowler, H.J.; Burton, A.; Hollis, J.M.; Reichenberger, S.; Jarvis, N.J. Identification of key climatic factors regulating the transport of pesticides in leaching and to tile drains. *Pest Manag. Sci. Former. Pestic. Sci.* **2008**, *64*, 933–944. [CrossRef]
44. Li, W.; Tao, C.; Ter Horst, M. Establishing surface and groundwater scenarios to assess pesticide environmental risk in China with a GIS spatial technique. *Abstr. Pap. Am. Chem. Soc.* **2014**, *248*, 1155.
45. Van Alphen, B.; Stoorvogel, J. Effects of soil variability and weather conditions on pesticide leaching—A farm-level evaluation. *J. Environ. Qual.* **2002**, *31*, 797–805.
46. de Berg, M.; Katz, M.J.; van der Stappen, A.F.; Vleugels, J. Realistic input models for geometric algorithms. *Algorithmica* **2002**, *34*, 81–97. [CrossRef]
47. Chen, L.-C.; Wu, C.-H.; Shen, T.-S.; Chou, C.-C. The application of geometric network models and building information models in geospatial environments for fire-fighting simulations. *Comput. Environ. Urban Syst.* **2014**, *45*, 1–12. [CrossRef]
48. Rahman, S.S.A.; Maulud, K.A. Approaching BIM-GIS Integration for 3D Evacuation Planning Requirement Using Multipatch Geometry Data Format. In *IOP Conference Series: Earth and Environmental Science*; IOP Publishing: Bristol, UK, 2019; Volume 385, p. 012033.
49. Zhu, J.; Wang, X.; Chen, M.; Wu, P.; Kim, M.J. Integration of BIM and GIS: IFC geometry transformation to shapefile using enhanced open-source approach. *Autom. Constr.* **2019**, *106*, 102859. [CrossRef]
50. Li, Y.; Soleimani, H.; Zohal, M. An improved ant colony optimization algorithm for the multi-depot green vehicle routing problem with multiple objectives. *J. Clean. Prod.* **2019**, *227*, 1161–1172. [CrossRef]